Proceedings of the XII International Symposium on Dynamic Problems of Mechanics (DINAME 2007),
P.S.Varoto and M.A.Trindade (editors), ABCM, Ilhabela, SP, Brazil, February 26 - March 2, 2007

Numerical analyses of the deformation behavior of cylinders undergoing Taylor impact tests

Larissa Driemeier[1] **and Michael Brünig**[2]

[1] Group of Solid Mechanics and Structural Impact, Department of Mechatronics and Mechanical Systems Engineering, University of São Paulo, Av. Prof. Mello Moraes 2231, São Paulo - SP - 05508-900, Brazil

[2] Lehrstuhl für Baumechanik - Statik, Universität Dortmund, August-Schmidt-Str. 6, D-44221 Dortmund, Germany

Abstract: The presentation discusses some aspects in the numerical simulation of Taylor impact tests. This requires the formulation of a rate-dependent thermoelastoplasticity approach at finite strains. The constitutive model consists of thermo-hyperelastic equations for the stresses and an evolution equation for the plastic internal variable. High strain rate thermoplastic material functions are proposed and parameters are identified by curve fitting of Hopkinson-bar-experiments with stainless steel specimens taking into account a wide range of strain rates and temperatures. Taylor impact tests of stainless steel cylinders are numerically simulated using the explicit finite element program LS-DYNA augmented by an user-defined material subroutine. The effect of variation of selected model parameters is discussed. Numerical results allow new interpretations of experimental observations and test data and give advice on identification of material parameters in rate-dependent inelastic constitutive models.

Keywords: Taylor test, impact, rate-dependent plasticity, numerical simulation

INTRODUCTION

Modern engineering technologies have placed increasing demands for constitutive modelling and the knowledge of material parameters at high strain rates of the order of $10^4 - 10^6 s^{-1}$. These rates are achieved, for example, in Taylor impact tests, where deformable flat-nosed cylinders are fired against fixed quasi-rigid walls. From experimental point of view this cylinder impact test is simple, inexpensive, and exhibits large strains, high strain rates, and elevated temperatures. Numerical analyses (see e.g. Brünig and Driemeier, 2006), however, have shown that these parameters vary throughout the specimen and throughout the duration of the test which leads to difficulties in identification of highly rate-dependent material parameters. Nevertheless, the Taylor test is often used to validate high-strain rate material constants under dynamic loading conditions or to demonstrate the quality of numerical codes in computational mechanics.

Based on impact experiments with cylinders Taylor (1948) estimated the dynamic yield stress of specimens using one-dimensional analysis which, however, does not provide the information necessary for description of high-strain rate dependent material behavior. Therefore, several improvements in the interpretation of Taylor impact test data and in one-dimensional analytical models extracting material property information from experimental results have been offered (see e.g. Maudlin et al., 1997; Jones et al., 1997, 1998). On the other hand, since large inelastic deformations, high strain rates and elevated temperatures occur these tests are also used to verify rate-dependent constitutive models under adiabatic conditions by comparing numerical predictions with experimental data (see e.g. Rule, 1997; Rohr et al., 2003, 2005). In this context, Taylor test results are used to validate or to estimate coefficients for phenomenological strength models needed for simulating dynamic loading processes using inverse identification procedures.

Furthermore, phenomenological modelling of thermomechanical processes for rate-dependent elastic-plastic solids involves appropriate statement of balance laws, first and second law of thermodynamics as well as constitutive equations for large rate-dependent elastic-plastic strains at elevated temperatures which may be useful for application to the analysis of adiabatic deformations. Thermo-elastic-plastic frameworks involving large strains have been developed particularly with respect to the phenomenological description of the deformation behavior of metals (see e.g. Green and Naghdi, 1965; Anand, 1985; Brown et al., 1989; Khan and Huang, 1992; Miehe, 1995; Khan et al., 2004; Brünig and Driemeier, 2006). The prediction of such complex thermomechanical processes can only be satisfactorily performed using numerical techniques such as the finite element method for solving the strongly coupled mechanical and thermal boundary value problems (see e.g. Argyris and Doltsinis, 1981; Belytschko et al., 1991; Simo and Miehe, 1992; Fotiu and Nemat-Nasser, 1996; Voyiadjis and Abed, 2006).

Currently many computer codes exist which can be used to perform computations of complex structures under dynamic loading conditions like intense impulsive loading due to high-velocity impact or explosive detonation. Within the context of phenomenological modelling this requires constitutive equations which describe the rate-dependent plastic behavior of metals as a function of strains, strain rates and temperature as well as corresponding procedures to identify the parameters for these approaches. For example, due to simplicity and availability of material coefficients many numerical simulations are based on the simple Johnson-Cook material model (Johnson and Cook, 1983) which accounts for isotropic strain

hardening, strain rate sensitivity, and thermal softening in an uncoupled form in one single equation. Rohr et al. (2005), however, have shown that the Johnson-Cook model might lead to questionable results in the high dynamic region and, thus, there is the necessity of more reliable and adequate material models.

The present paper discusses the formulation of a rate-dependent thermoplasticity approach at finite strains. Based on experimental measurements on stainless steel (Nemat-Nasser et al., 2001) phenomenological thermoplastic constitutive functions are proposed and corresponding material parameters are identified. Taylor impact tests with specimens of this material are numerically simulated using the explicit finite element program LS-DYNA augmented by an user-defined material subroutine and the effect of variation of selected model parameters is discussed. Numerical results allow new interpretations of experimental observations and test data and give advice on identification of some material parameters in rate-dependent inelastic constitutive models.

CONSTITUTIVE MODEL

The rate-dependent theoretical framework presented by Brünig and Driemeier (2006) is used to describe the high strain rate and temperature dependent inelastic deformation behavior of ductile metals. Briefly, the finite thermo-elastic part of the material behavior is assumed to be governed by the Helmholtz free energy function

$$\rho_o\,\phi^{el}(\mathbf{A}^{el},\Theta) = G\;\mathbf{A}^{el}\cdot\mathbf{A}^{el} + \frac{1}{2}(K-\frac{2}{3}G)\;(\mathrm{tr}\mathbf{A}^{el})^2 - 3K\,\alpha_T\,(\Theta-\Theta_o)\,\mathrm{tr}\mathbf{A}^{el} + \rho_o\,h(\Theta) \tag{1}$$

where $\mathbf{A}^{el}$ is the elastic Almansi strain tensor, G and K represent the shear and bulk modulus of the material, α_T is the coefficient of thermal expansion and $h(\Theta)$ denotes an explicit function of temperature. Taking into account hyperelastic constitutive relationship the stress tensor is expressed in the form

$$\mathbf{T} = 2G\,\mathbf{A}^{el} + (K-\frac{2}{3}G)\,\mathrm{tr}\mathbf{A}^{el}\;\mathbf{1} - 3K\,\alpha_T\,(\Theta-\Theta_o)\,\mathbf{1}\,. \tag{2}$$

If any effect of plastic straining on the finite thermo-elastic material behavior is neglected, the associated tensor of elastic moduli is determined from

$$\mathscr{C}^{el} = \rho_o\,\frac{\partial^2\phi^{el}}{\partial\mathbf{A}^{el}\otimes\partial\mathbf{A}^{el}} = 2G\;\mathscr{I} + (K-\frac{2}{3}G)\,\mathbf{1}\otimes\mathbf{1} \tag{3}$$

with the fourth order identity tensor

$$\mathscr{I} = \delta^i_k\,\delta^l_j\,\mathbf{g}_i\otimes\mathbf{g}^j\otimes\mathbf{g}_l\otimes\mathbf{g}^k\,. \tag{4}$$

In elastic-plastically deformed metals volumetric plastic strains are negligible (Spitzig et al., 1975), and, thus, the plastic potential function

$$g^{pl}(\mathbf{T},\gamma,\Theta) = \sqrt{J_2} - \overline{c}(\gamma,\Theta) \tag{5}$$

depends on the second invariant of the stress deviator $J_2 = \frac{1}{2}\,\mathrm{dev}\mathbf{T}\cdot\mathrm{dev}\mathbf{T}$ and on the temperature-dependent equivalent stress $\overline{c}(\gamma,\Theta)$. This leads to the isochoric plastic strain rate

$$\dot{\mathbf{H}}^{pl} = \dot\lambda\;\frac{\partial g^{pl}}{\partial\mathbf{T}} = \dot\lambda\;\frac{1}{2\sqrt{J_2}}\,\mathrm{dev}\mathbf{T} = \dot\gamma\mathbf{N} \tag{6}$$

where $\dot\lambda$ is a non-negative scalar-valued factor, $\mathbf{N} = \frac{1}{\sqrt{2\,J_2}}\,\mathrm{dev}\mathbf{T}$ denotes the normalized deviatoric tensor and $\dot\gamma = \mathbf{N}\cdot\dot{\mathbf{H}}^{pl} = \frac{1}{\sqrt{2}}\,\dot\lambda$ represents the equivalent plastic strain rate.

Based on the experiments presented by Spitzig et al. (1975, 1976, 1984) showing the hydrostatic stress dependence of yield strength even in metal plasticity and following the corresponding elastic-plastic continuum model proposed by Brünig (1999) the equivalent stress c may be adequately described by the relation

$$c = a\,I_1 + \sqrt{J_2} \tag{7}$$

where a represents the hydrostatic stress coefficient and $I_1 = \mathrm{tr}\mathbf{T}$ is the first invariant of the stress tensor $\mathbf{T}$. The coefficients, a and c, are strain-dependent, whereas experimental data have shown that the ratio $\alpha = a/c$ is constant. The equivalent stress (7) can alternatively be written in the form

$$c = \frac{1}{1-\alpha I_1}\,\sqrt{J_2}\,. \tag{8}$$

Furthermore, the equivalent stress is expressed as a specific function of the equivalent plastic strain, equivalent plastic strain rate and temperature:

$$c(\gamma,\dot\gamma,\Theta) = \sigma(\gamma)\;\;f_1(\dot\gamma)\;\;f_2(\Theta-\Theta_o) \tag{9}$$

which is assumed on the basis of empirical arguments (see e.g. Litonski, 1977; Johnson and Cook, 1983; Johnson et al., 1983; Klopp et al., 1985; Zerilli and Armstrong, 1987). In Eq. (9) the reference stress $\sigma(\gamma)$ represents the averaged isotropic resistance to macroscopic plastic flow offered by the internal state of the material. It is determined using quasistatic tests at constant reference temperature Θ_o. For example, the reference stress $\sigma(\gamma)$ can be numerically simulated by the power law

$$\sigma(\gamma) = \sigma_o(\frac{H_o\,\gamma}{n\,\sigma_o} + 1)^n \tag{10}$$

where σ_o denotes the initial yield stress, H_o represents the initial hardening modulus and n means the hardening exponent.

The experimentally observed increasing dependence of the equivalent stress on the inelastic strain rate $\dot{\gamma}$ is described by the strain rate hardening function $f_1(\dot{\gamma})$ which can be obtained from a series of dynamic experiments at different strain rates and reference temperature. The rate-dependent motion of dislocations on the microscale is macroscopically modelled by the power law function

$$f_1(\dot{\gamma}) = 1 + d(\frac{\dot{\gamma} - \dot{\gamma}_o}{\dot{\gamma}_o})^m \tag{11}$$

where d and m are constitutive parameters which have to be determined by the experiments described above and the reference inelastic strain rate $\dot{\gamma}_o$ is given by the quasistatic reference test.

In addition, the decrease in equivalent stress with increasing temperature as observed in experiments is taken into account by the thermal softening function $f_2(\Theta - \Theta_o)$ with $f_2(0) = 1$ which can be determined from a series of isothermal tests at different temperatures Θ and constant strain rates. The thermal softening behavior is numerically modelled by the power law of the form

$$f_2(\Theta - \Theta_o) = 1 - b(\frac{\Theta - \Theta_o}{\Theta_m})^q \tag{12}$$

where b and q are constitutive parameters which have to be determined by fitting the numerical model to experimental data and Θ_m denotes the melting temperature.

IMPLEMENTATION

The numerical algorithm of the theory presented above has been implemented, in Fortran, into the explicit finite element code LS-DYNA through the use of the user defined subroutine (UMAT) option. The routine is designed to work with solid elements, all of the material constants are entered into the input deck. The history variables for the finite element analysis are defined to include the deviatoric stresses, the hydrostatic stress, the values of the state variables and the inelastic strain tensor. The numerical integration of the evolution equations of the respective inelastic strain rate tensors over the considered time increment is performed by a generalized version of the inelastic predictor method (see Brünig, 2001).

TAYLOR IMPACT TESTS

The high-rate deformation behavior of ductile cylinders undergoing Taylor impact tests will be numerically simulated and the effect of various parameters on the specimen's adiabatic deformation process will be analyzed in detail.

Material parameters

Nemat-Nasser et al. (2001) performed uniaxial compression tests on cylindrical samples to investigate the thermomechanical behavior of AL-6XN stainless steel. They performed systematic compression experiments at low-to-high-strain rates and over a wide range of temperatures. Based on these experimental data, the following parameters based on the power law (10) can be obtained: $\sigma_0 = 150$ MPa, $H_0 = 18000$ MPa and $n = 0.313$ whereas the strain-rate-dependent function (11) takes into account $d = 0.02$ and $m = 0.12$, and the material parameters of the temperature dependent function (12) are chosen to be $b = 0.69$ and $q = 0.49$ with the melting temperature $\Theta_m = 1673$ K. In addition, the hydrostatic stress parameter (see Eq. (8)) is taken to be $a/c = 0.000023$ MPa^{-1} which is a realistic value for many steels (Spitzig et al., 1976). The elastic parameters are the shear modulus $G = 81$ GPa and the bulk modulus $K = 166$ GPa. Furthermore, based on the results presented by Rosakis et al. (2000) the fraction of the rate of plastic work converted into heat is assumed to be 0.5 which has been shown by Brünig and Driemeier (2006) to be a realistic approximation for Taylor tests with this material.

Numerical simulations

The numerical simulations on Taylor impact tests are based on the material parameters discussed above. Eight-node 3D solid elements with one-point integration and stiffness-based hourglass control are used to discretize the cylindrical specimens. The numerical model taking into account a quarter of the cylindrical specimen consists of 8800 elements, as shown in Fig.1. The ratio of initial length L_o and initial diameter D_o is taken to be 5.0. Fine mesh is generated in the front part of the cylinder where large inelastic deformations are expected to occur while relatively coarse discretization is

used in the rear part which is expected to remain nearly undeformed. The cylinder is launched against a quasi-rigid wall with an initial velocity of 450 m/s, which has been shown by Brünig and Driemeier (2006) to lead to characteristic impact deformations. The typical time step size was at the order of 10^{-8} s in all numerical calculations.

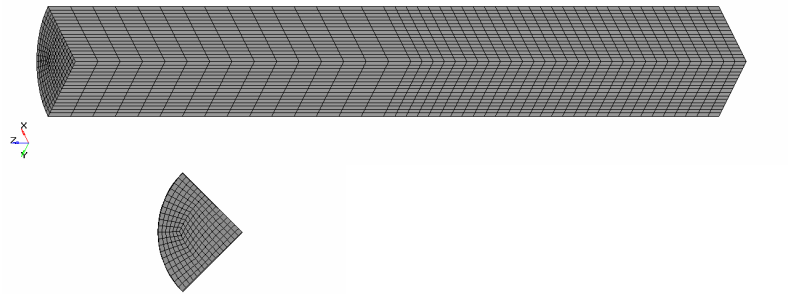

Figure 1 – Finite element mesh of the specimen.

Similar to other numerical simulations of Taylor tests (Maudlin et al., 2003; Zaera and Fernandez-Saez, 2006) frictionless contact conditions between the front surface of the cylinders fabricated of AL-6XN stainless steel and the rigid target is assumed. Since the assumptions of a rigid wall and this friction parameter might seem to be arbitrary, the effects of the variation of these parameters on the specimen's behavior will be discussed in the following subsections.

Figure 2 shows the final deformed specimen after Taylor test. Remarkable deformations predicted in the contact region are characteristic for these cylinder impact experiments. The maximum axial strain rates are between $4 \cdot 10^4$ 1/s and $6.5 \cdot 10^5$ 1/s which are in the desired range. It should be noted that in contrast to other numerical simulations reported, for example, by Rule (1997), Johnson and Holmquist (1988) and Rohr et al. (2003, 2005) these results show the bulge area near the mushroomed end which has been measured in many experiments (see e.g. Jones et al., 1997; Maudlin et al., 2003).

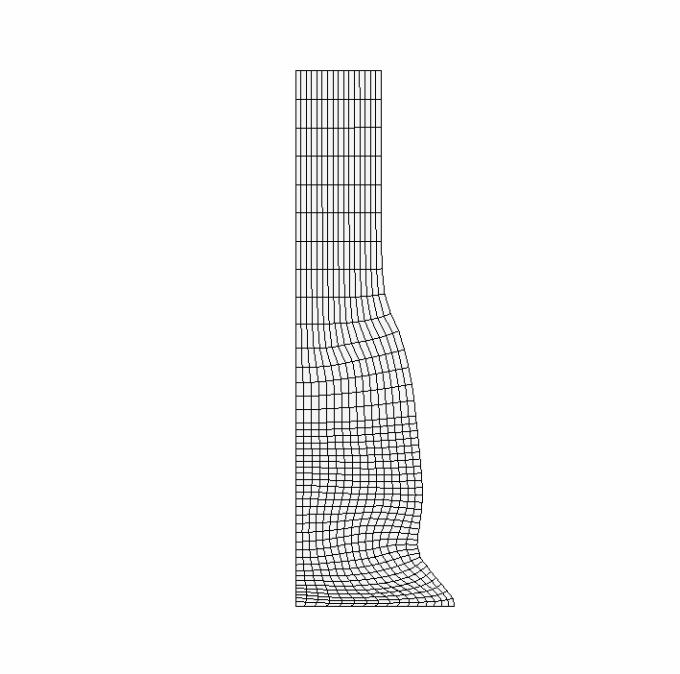

Figure 2 – Deformed mesh

The evolution of axial strain rates in the center of the specimen's foot is shown in Fig. 3. In particular, shortly after impact high axial compression strain rates up to $6.5 \cdot 10^5$ 1/s are observed which remarkably vary throughout the duration of the test and quickly decrease. Figure clearly shows that high axial strain rates in the foot area only occur shortly after the onset of impact and after 20 μs the rates are nearly zero. As has been discussed by Brünig and Driemeier (2006) in shorter specimens, however, further waves with moderate axial strain rates may occur after this section of zero strain rates which also can be observed here 40 μs after the onset of impact, but the additional maximum strain rates are only $2 \cdot 10^5$ 1/s.

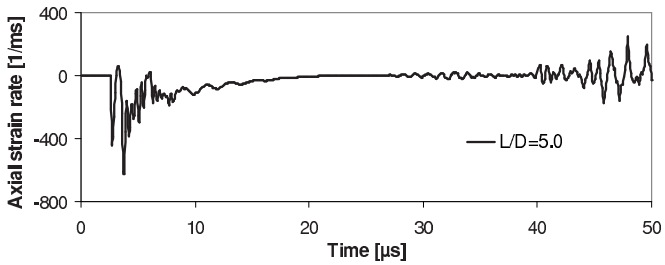

Figure 3 – Axial strain rate vs. time.

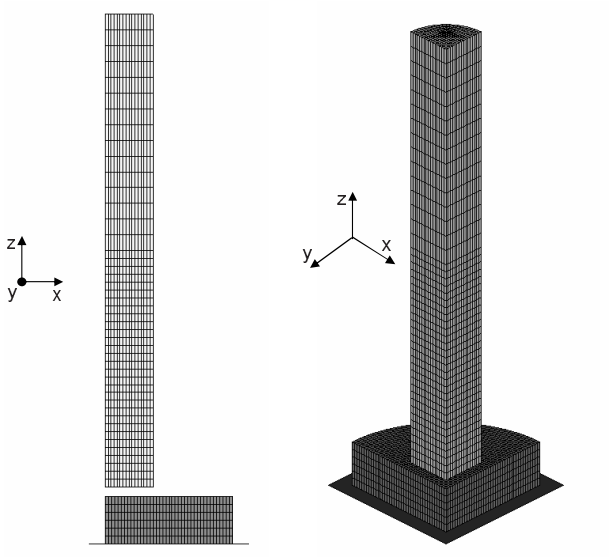

Figure 4 – Finite element meshes for the specimen and the plate.

The numerically predicted behavior of the long specimen agrees quite well with the analysis of Jones et al. (1997) who characterized the deformation process of the impacted cylinder by different phases. In their opinion, the early time behavior (Phase I) is shock dominated nonlinear motion of the plastic wave front with high strain rates initiated by the impact. It is followed by a period (Phase II) with the attenuation of shock waves and lower strain-rate plastic deformations characterized by plastic waves propagating at a uniform speed. The duration of this period depends on several parameters but most importantly on the length of the undeformed section after Phase I deformation. All of the physical parameters in the problem are virtually constant during Phase II deformation. In a third regime (Phase III) deceleration of the plastic wave front occurs and its velocity must come to zero at the end of the event.

Numerical studies on the wall stiffness

In Taylor experiments, cylinders are fired against a very stiff plate which is fixed in a sabot. Usually, numerical analyses are based on the assumption of a rigid target but in this subsection elastic-plastic material properties of the wall are taken into account to be able to study the effect of the stiffness of the plate on the numerically predicted behavior of the impacted cylinder. In particular, the target is chosen to be a plate made of a tool steel material with thickness of 3mm, 5mm, 7mm and 10mm, respectively, and the border is clamped into a rigid sabot. The finite element meshes of the cylinder and the plate are shown in Fig. 4.

Tool steels typically have excess carbon alloys which make them hard and wear-resistant. Most tool steels are used in a heat-treated state, generally hardened and tempered. The elastic-plastic behavior of this material is modelled by the constitutive approach discussed above using the parameters $G = 117$ GPa, $K = 253$ GPa, $\sigma_0 = 1539$ MPa, $H_0 = 7000$ MPa and $n = 0.1$.

Deformed configurations and distributions of equivalent plastic strains of the cylinders fired against a rigid wall and against an elastic-plastic plate of 5mm thickness fixed in a rigid sabot are shown in Fig. 5. The deformation modes are very similar, the cylinder fired against the stiff plate show non-flat deformations in the foot area as well as smaller foot diameter. The equivalent plastic strains are lower in the foot area whereas their further distributions are very similar. The effect of wall stiffness on the final geometry of the impacted cylinders is quantified in Fig. 6. In particular, the stiffness

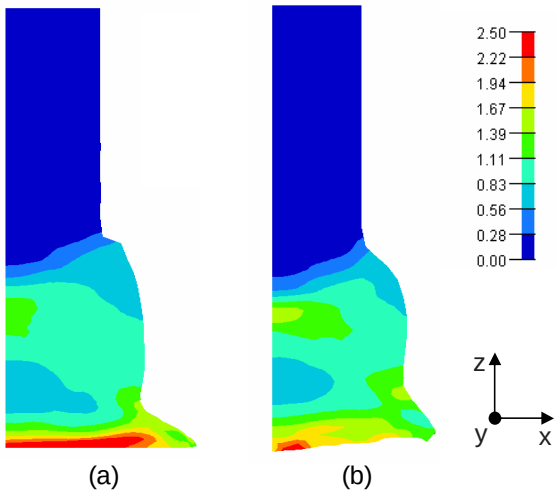

Figure 5 – Equivalent plastic strains for (a) rigid wall and (b) plate with 5mm thickness.

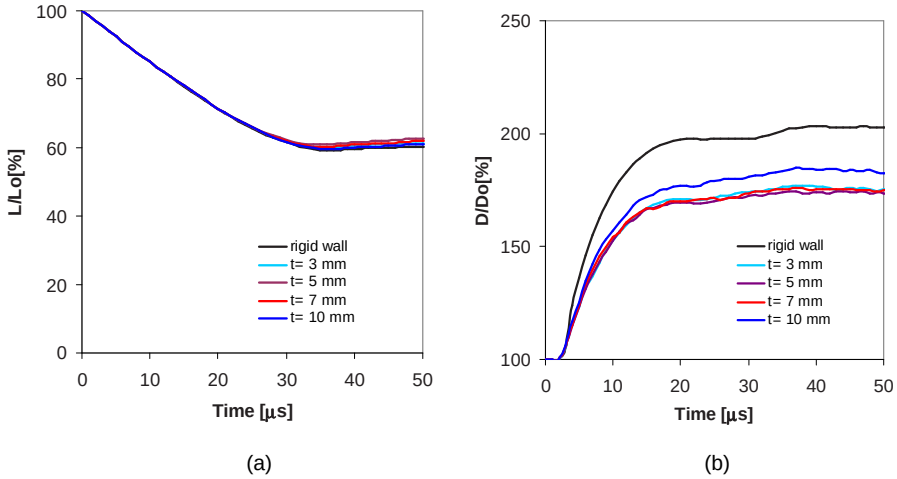

Figure 6 – Evolution of length and foot diameter for different plate thickness.

of the plate does not affect the final length of the deformed specimens but has an influence of the diameter of the foot. The final diameter of the cylinder fired against the rigid wall is numerically predicted to be about 200% of its initial value while that one fired against a stiff plate of 10mm thickness only reaches 185%. Smaller increases in foot diameter of about 175% have been obtained for smaller plates. It should be noted that the plates remain nearly elastic during impact, only the one with 3mm thickness showed remarkable plastic deformations.

Numerical studies on the friction coefficient

It is well known that friction between the cylinder and the target mainly depends on the initial velocity but friction parameters are not strongly explored or experimentally quantified in the open literature about Taylor tests. For example, some authors use $f = 0.10$ (Rohr et al., 2005; Teng et al., 2005) whereas others base their numerical analyses on friction-less contact conditions $f = 0.0$ (see Maudlin et al., 2003; Zaera and Fernandez-Saez, 2006) without further explanations. In order to more elucidate this problem, the effect of different friction parameters on the inelastic deformation behavior of impacted cylinders will be studied in the present paper. The numerical calculations are based on $f = 0.; 0.01$ and 0.1.

The effect of assumed friction coefficients on the final specimen's geometry is shown in Fig. 7. In particular, the numerical simulation based on $f = 0.1$ leads to an increase in foot diameter of about 80% whereas the calculations with $f = 0.01$ and $f = 0.$ predict similar final diameters which are about twice the initial value. Concerning the final length, however, no remarkable differences are obtained for all considered coefficients and it seems to be nearly unaffected by the assumed friction parameters. These effects can be also seen in Fig. 8. Smaller friction leads to more pronounced bulge area and dominant concentration of plastic deformations near the contact zone. For example, the equivalent plastic strains in the center of the foot area are of about 3.1. The numerical simulations based on $f = 0.1$, on the other hand,

numerically predicts more smooth bulge area and less concentrated inelastic deformations. Lower equivalent plastic strains are obtained in the contact zone which only reach 200%.

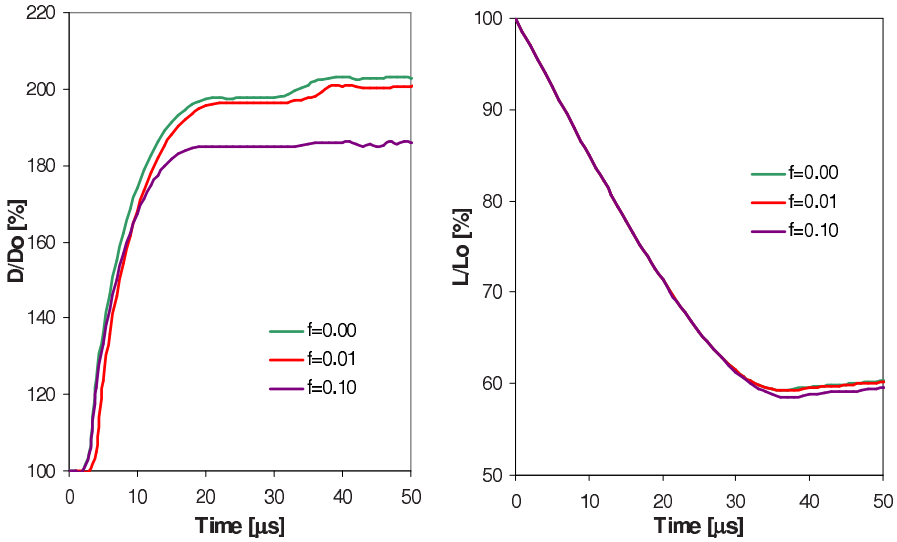

Figure 7 – Evolution of length and foot diameter for different friction parameters f.

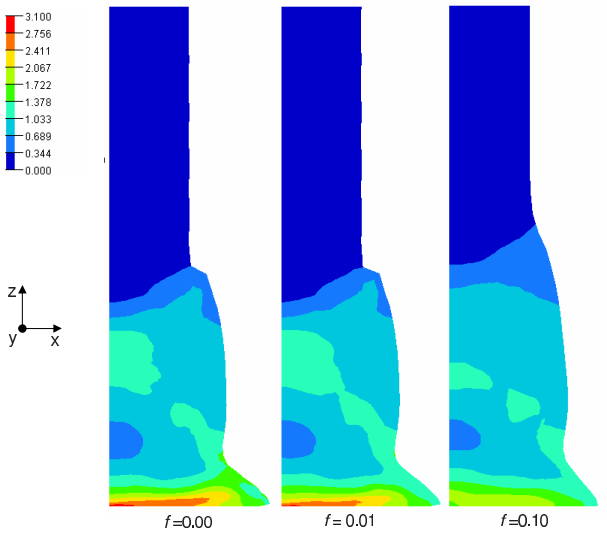

Figure 8 – Deformed configurations and distribution of the equivalent plastic strain for different f.

These numerical calculations have shown that small friction coefficients do not remarkably affect the numerical results. Thus, simulations dealing with high initial specimen's velocities could be realistically performed with zero friction, small values are allowed if this will lead to numerical advantages like more stable algorithms or lower computation time. Numerical analyses taking into account lower initial velocities, on the other hand, are recommended to use friction parameters up to $f = 0.1$ but the realistic coefficient could be experimentally controlled by the final specimen's geometry.

CONCLUSIONS

Some aspects in the numerical analyses of Taylor impact tests have been discussed. In the paper's theoretical part a macroscopic rate-dependent constitutive model has been presented and thermoplastic material functions have been proposed. Based on this approach Taylor impact tests have been numerically simulated using the explicit finite element program LS-DYNA augmented by an user-defined material subroutine.

The effect of variation of selected model parameters has been discussed and might lead to more realistic assumptions in numerical simulations of impact problems. For example, the concept of a rigid target in cylinder impact tests with high initial velocities up to 450 m/s might lead to unrealistically large equivalent plastic strains and final deformations

of the specimens and should only be used for metal cylinders characterized by low initial yield stresses. If, however, steel specimens with higher initial yield strengths are tested the numerical simulations should be based on stiff walls with plates of more than 5mm thickness fixed in a quasi-rigid sabot. Furthermore, the identification of friction coefficients has been elucidated and zero friction is recommended in numerical simulations dealing with high initial velocities whereas coefficients up to 0.1 should be taken into account for less high deformation rate tests.

REFERENCES

Anand, L.,1985. Constitutive equations for hot-working of metals. Int. J. Plasticity 1, 213-231.

Argyris, J.H., Doltsinis, J.S., 1981. On the natural formulation and analysis of large deformation coupled thermomechanical problems. Comp. Meth. Appl. Mech. Eng. 25, 195-253.

Belytschko, T., Moran, B., Kulkarni, M., 1991. On the crucial role of imperfections in quasi-static viscoplastic solutions. J. Appl. Mech. 58, 658-665.

Brown, S.T., Kim, K.H., Anand, L., 1989. An internal variable constitutive model for hot working of metals. Int. J. Plasticity 5, 95-130.

Brünig, M., 1999. Numerical simulation of the large elastic-plastic deformation behavior of hydrostatic stress-sensitive solids. Int. J. Plasticity 15, 1237-1264.

Brünig, M., 2001. Numerical analysis and large strain elastic-viscoplastic behavior of hydrostatic stress-sensitive metals. Int. J. Solids Structures 38, 635-656.

Brünig, M., Driemeier, L., 2006. Numerical simulation of Taylor impact tests. Int. J. Plasticity (submitted for publication).

Fotiu, P.A., Nemat-Nasser, S., 1996. A universial integration algorithm for rate-dependent elastoplasticity. Comput. Struct. 59, 1173-1184.

Green, A.E., Naghdi, P.M., 1965. A general theory of an elasto-plastic continuum. Arch. Rat. Mech. Anal. 18, 251-281.

Johnson, G.R., Cook, W.H., 1983. A constitutive model and data for metals subjected to large strains, high strain rates and high temperatures. In: Proc. 7th Int. Symp. Ballistics, The Hague, Netherlands, 541-547.

Johnson, G.R., Hoegfeldt, J.M., Lindholm, U.S., Nagy, A., 1983. Response of various metals to large torsional strains over a large range of strain rates – I: Ductile metals. J. Eng. Mater. Technol. 105, 42-47.

Johnson, G.R., Holmquist, T.J., 1988. Evaluation of cylinder-impact test data for constitutive model constants. J. Appl. Phys. 64, 3901-3910.

Jones, S.E., Drinkard, J.A., Rule, W.K., Wilson, L.L., 1998. An elementary theory for the Taylor impact test. Int. J. Impact Engng. 21, 1-13.

Jones, S.E., Maudlin, P.J., Forster, J.C., 1997. An engineering analysis of plastic wave propagation in the Taylor test. Int. J. Impact Engng. 19, 95-106.

Khan, A.S., Huang, S., 1992. Experimental and theoretical study of mechanical behavior of 1100 aluminum in the range $10^{-5} - 10^{4}\mathrm{s}^{-1}$. Int. J. Plasticity 8, 397-424.

Khan, A.S., Suh, Y.S., Kazmi, R., 2004. Quasi-static and dynamic loading responses and constitutive modeling of titanium alloys. Int. J. Plasticity 20, 2233-2248.

Klopp, R.W., Clifton, R.J., Shawki, T.G., 1985. Pressure-shear impact and the dynamic viscoplastic response of metals. Mech. Mater. 4, 375-385.

Litonski, J., 1977. Plastic flow of a tube under adiabatic torsion. Bull. Acad. Pol. Sci. Ser. Sci. Tech. 25, 7-14.

Maudlin, P.J., Bingert, J.F., Gray III, G.T., 2003. Low-symmetry plastic deformation in BCC tantalum: experimental observations, modeling and simulations. Int. J. Plasticity 19, 483-515.

Maudlin, P.J., Foster, J.C., Jones, S.E., 1997. A continuum mechanics code analysis of steady plastic wave propagation in the Taylor test. Int. J. Impact Engng. 19, 231-256.

Miehe, C., 1995. A theory of large-strain isotropic thermoplasticity based on metric transformation tensors. Arch. Appl. Mech. 66, 45-64.

Nemat-Nasser, S., Guo, W.G., Kihl, D.P., 2001. Thermomechanical response of AL-6XN stainless steel over a wide range of strain rates and temperatures. J. Mech. Phys. Solids 49, 1823-1846.

Rohr, L., Nahme, H., Thoma, K., 2003. A modified Taylor-test in combination with numerical simulations – a new approach for the determination of model parameters under dynamic loads. J. Phys. IV 110, 513-518.

Rohr, L., Nahme, H., Thoma, K., 2005. Material characterization and constitutive modelling of ductile high strength steel for a wide range of strain rates. Int. J. Impact Engng. 31, 401-433.

Rule, W.K., 1997. A numerical scheme for extracting strength model coefficients from Taylor test data. Int. J. Impact Engng. 19, 797-810.

Simo, J.C., Miehe, C., 1992. Associative coupled thermoplasticity at finite strains: Formulation, numerical analysis and implementation. Comp. Meth. Appl. Mech. Eng. 98, 41-104.

Spitzig, W.A., Richmond, O., 1984. The effect of pressure on the flow stress of metals. Acta Metall. 32, 457-463.

Spitzig, W.A., Sober, R.J., Richmond, O., 1975. Pressure dependence of yielding and associated volume expansion in tempered martensite. Acta Metall. 23, 885-893.

Spitzig, W.A., Sober, R.J., Richmond, O., 1976. The effect of hydrostatic pressure on the deformation behavior of maraging and HY-80 steels and its implications for plasticity theory. Metall. Trans. A 7A, 1703-1710.

Taylor, G.I., 1948. The use of flat-ended projectiles for determining dynamic yield stress, I. Theoretical considerations. Proc. Roy. Soc. London A-194, 289-299.

Teng, X., Wierzbicki, T., Hiermaier, S., Rohr, I., 2005. Numerical prediction of fracture in the Taylor test. Int. J. Solids Struct. 42, 2929-2948.

Voyiadjis, G.Z., Abed, F.H., 2006. A coupled temperature and strain rate dependent yield function for dynamic deformations of bcc metals. Int. J. Plasticity 22, 1398-1431.

Zaera, R., Fernandez-Saez, J., 2006. An implicit consistent algorithm for the integration of thermoviscoplastic constitutive equations in adiabatic conditions and finite deformations. Int. J. Solids Structures 43, 1594-1612.

Zerilli, F.J., Armstrong, R.W., 1987. Dislocation-mechanics-based constitutive relations for material dynamics calculations. J. Appl. Phys. 61, 1816-1825.